2026 IEEE International Conference on Robotics and Automation (ICRA 2026)
June 1-5, 2026. Vienna, Austria

Explicit Analytical Derivation of LSL and RSR Dubins' Paths for Intercepting a Uniformly Moving Target

Titouan Belier[1], Lionel Lapierre[1], Christophe Viel[2], Loïck Degorre[3], Damien Massé[4] ,

***Abstract*— Autonomous underwater robotics faces significant challenges, particularly in the reliable recovery of Autonomous Underwater Vehicles (AUVs) after mission completion. To address this, small AUVs can dock onto a moving mothership for safe transport to recovery sites, reducing operational risks. This paper presents an explicit analytical derivation of the LSL (Left-Straight-Left) and RSR (Right-Straight-Right) Dubins' Paths for intercepting an uniformly moving target, a critical problem for robust rendezvous in dynamic marine and underwater environments. The proposed approach leverages the classical Dubins' Path model to generate time optimal, real-time, curvature-constrained paths suitable for 2D AUVs. Experimental validation on an Unmanned Surface Vehicle (USV) demonstrates the effectiveness of the developed motion planning strategy.**

I. Introduction

Autonomous underwater robotics is a particularly challenging field. One of the main constraints for the deployment of Autonomous Underwater Vehicles (AUVs) in open sea environments is the difficulty to recover them at the end of their missions. An effective method to simplify recovery is to dock small AUVs onto a larger mothership, which then transports them to the recovery site [1] [2].

This concept offers autonomy as no operator is needed during the mission. However, docking these vehicles while the mothership is in motion requires the development of robust rendezvous and interception strategies. Motion planning is then crucial to enable the AUVs to effectively intercept and dock to the moving target.

The field of path planning is extensively studied in robotics, with many approaches designed to generate the fastest paths that respect the dynamic constraints of vehicles [3]. Among these, the Dubins' Path model [4] is a classical reference for generating minimum-curvature path from static origin to static goal with velocity and heading constraints. Making it particularly suitable for aerial and underwater vehicles. The work of [5] derived a solution to this problem for vehicles that goes both forwards and backwards.

Separately, an alternative proof based on Pontryagin's Maximum Principle [6] for constructing a sufficient family of solutions, has been presented in [7].

This problem has been extended to reach a 3D fixed pose with Dubins path. In [8], the authors propose the use of helical paths, defined by maximum pitch and yaw angles, allowing the vehicle to gradually reach the target altitude (or depth). Subsequently, [9] introduces an additional constraint on the maximum allowable curvature of the vehicle, in order to better reflect physical limitations. However, the integration of this constraint leads to significantly longer paths. More recently, [10] presents a new algorithm selecting the most suitable strategy between the two previous approaches: the resulting path satisfies the vehicle's physical constraints while maintaining a reasonable length.

The objective in our case is to reach a 2D moving target. Some studies discuss the shortest relaxed Dubins' Path without considering final heading, such as [11]. Other papers compute the shortest paths to reach a 2D fixed geometrical path such as a circle in [12]. However, in our scenario, the mothership is moving at a constant speed and heading. This situation is therefore closer to a pursuer-target interception problem, where the goal is to intercept a dynamic target as presented in [13]. To the authors' best knowledge, no paper has addressed this problem without relying on a numerical solver. Such an approach may introduce computational delays that hinder real-time implementation on low-power CPUs. A typical mission in this context is illustrated on Fig. 1.

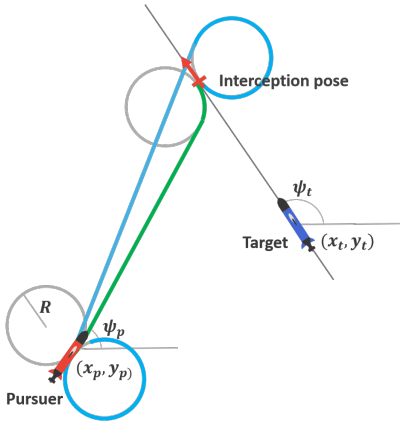

Fig. 1: Summary illustration of the proposed approach

Therefore, this paper presents an explicit analytical solution for a rendezvous problem using the Circle-Straight-Circle (CSC) Dubins' Paths, enabling real-time determination of the fastest path to reach the target with the same final heading. One of the main objective is to obtain a fast and light computation that could integrate the method into larger computational architectures, such as path planning or probabilistic methods.

*This work was supported by Agence de l'Innovation de Défense (AID)
[1] (corresponding author, name.surname@ensta.fr) Lab-STICC, ENSTA IP Paris, Brest, France
[2] CNRS and Lab-STICC, ENSTA IP Paris, Brest, France
[3] COSMER, Université de Toulon, Toulon, France
[4] Lab-STICC, Université de Bretagne Occidentale, Brest, France

The main contributions of this work are:

- an explicit and analytical expression for the LSL and RSR Dubins paths for the intersection of a target in uniform linear motion;
- an analytical, though implicit, expression for the Left-straight-Right (LSR) and Right-straight-Left (RSL) Dubins' paths for the intersection of a target in uniform linear motion;
- an experimental validation using two USVs to demonstrate the effectiveness of the proposed approach.

The paper is organized as follows. Section II introduces the problem description and statements. Section III presents the general resolution of the three subpaths. Section IV introduces the analytical solution for the LSL and RSR paths and gives an implicit solution for LSR and RSL ones. Section V presents the simulation and experimental results to prove the results and compare the computational delays of both cases. Section VI concludes the papers and discusses future perspectives.

II. Problem description

A. Notations

In a 2D inertial frame $\mathcal{R}$, let us consider a pursuer vehicle whose objective is to intercept a target vehicle. The following notations will be used throughout this paper:

- $X_p(t) = [x_p(t), y_p(t)]^T$: pursuer's position in $\mathcal{R}$;
- ψ_p: heading angle of the pursuer vehicle;
- v_p: norm of the longitudinal speed of the pursuer vehicle;
- R: minimum turning radius of the pursuer vehicle supposed fixed;
- $X_t(t) = [x_t(t), y_t(t)]^T$: target's position in $\mathcal{R}$;
- ψ_t: heading angle of the target vehicle;
- v_t: norm of the longitudinal speed of the target vehicle.

B. Problem statement

We aim to dock the pursuer behind the target, they must then meet with the exact same heading angle. The goal of this work is thus to determine the fastest interception path respecting this constraint.

The pursuer is an underactuated torpedo-shaped AUV. One convenient way in this context to control an AUV is to maintain a constant speed. This implies an inability to remain stationary underwater, in exchange for greater resilience to currents.

Consider that the target is moving from an initial position X_t^0 at time t_0 with constant velocity v_t and a constant heading ψ_t. Its trajectory follows:

$$X_t(t) = X_t^0 + v_t \begin{pmatrix} \cos(\psi_t) \\ \sin(\psi_t) \end{pmatrix} . (t - t_0) \tag{1}$$

One assumes that:

- v_p and v_t are constant and $v_p > v_t > 0$;
- X_t follows a straight line at constant speed, so $\psi_t = \psi_t(0) = \psi_t(t_f)$.

The dynamics of the pursuer vehicle can be expressed as

$$\begin{cases} \dot{X}_p(t) &= \begin{pmatrix} v_p \cos(\psi_p(t)) \\ v_p \sin(\psi_p(t)) \end{pmatrix} \\ \dot{\psi}_p(t) &= u(t) \end{cases} \tag{2}$$

where $u(t) \in \left[-\frac{R}{v_p}, \frac{R}{v_p}\right]$ is a control input, not described in this paper (see example [14]).

The problem considered in this work is defined as follows:

Definition 1: The pursuer vehicle reaches the target vehicle iff there exists a finite time $t_f < +\infty$ such that

$$\lim_{t \to t_f} \|X_t(t) - X_p(t)\| = 0 \tag{3}$$

and

$$\lim_{t \to t_f} \psi_p(t) = \psi_t(t) \tag{4}$$

C. Dubins' Path

The Dubins' Path framework is particularly relevant for vehicles with limited turning radius, making it suitable to model the motion of underactuated vehicles like AUVs.

The pose of a system is described by the triplet $\mathrm{F}(x, y, \psi)$, which encodes its position in the plane together with its orientation. The set of all possible configurations defines the space $\mathbb{R}^2 \times S^1$.

For this class of systems, it has been shown—first in [4] and later refined in [7]—that the shortest path between two given configurations always exists and necessarily belongs to a restricted set of six candidates. Each candidate path is composed of at most three elementary motions chosen among circular arcs of fixed radius denoted C and straight-line segments denoted S.

By calling respectively L, R and S the left (counterclockwise) turning circle, right (clockwise) turning circle and straight line, these six solutions can be grouped into two families:

- CSC family: consists of two arcs separated by a straight segment, yielding four possible patterns: *LSL*, *RSR*, *LSR*, and *RSL*.
- CCC family: consists of three consecutive circular arcs, with two possible patterns: *LRL* and *RLR*. In these cases, the intermediate arc spans an angle greater than π.

We consider here only the CSC solutions, for which we seek for an analytical solution. Although, this paper focuses only on the CSC family, CCC paths exist only if the distance between the initial and final positions is less than $4R$ (see [4]), which is rarely the case in the scenarios we study.

Hereafter, we denote C_1 and C_3 the first and second rotations performed, respectively, and S_2 as the straight segment executed between the two rotations. The symbol δ_k indicates the direction of rotation during C_k, $k \in \{1, 3\}$ such that:

- $\delta_k = 1$ if C_k is a counterclockwise rotation L;
- $\delta_k = -1$ if C_k is a clockwise rotation R.

III. General resolution

The objective is to minimize the time required for the pursuer to reach its target. Here, we consider the pursuer to move at a constant velocity and to turn with its minimum turning radius. Since the entire motion is executed at constant velocity, the Dubins path represents both the shortest and the fastest trajectory.

A. Dubins' Path Notations

Let's define the parameters that are specific to the Dubins' Path problem and their specific assumptions. The parameters are illustrated in Fig. 2.

- times t_0, t_1, t_2 and $t_3 = t_f$ where, t_0 is the initial time, t_1, t_2, t_3 are the times at the end of C_1, S_2 and C_3 respectively;
- $R_1 = R_3 = R$ the radii of C_1 and C_3;
- turning angles $\psi_k = \psi_p(t_k)$ of the pursuer associated to the times t_k with $k = \{0, 1, 2, 3\}$. Note that $\psi_0 = \psi_p(t_0)$ is known and $\psi_3 = \psi_p(t_3) = \psi_t$ since the heading of the two vehicles coincide when $t_3 = t_f$. During a straight segment followed between t_1 and t_2, one has $\psi_1 = \psi_2$
- $\alpha_1 = \psi_1 - \psi_0$ the angle swept by the vehicle during C_1;
- d_2 the distance traversed by the vehicle during S_2;
- $\alpha_3 = \psi_3 - \psi_2$ the angle swept by the vehicle during C_3.

Let $\alpha_k > 0$ if $\delta_k > 0$ and $\alpha_k < 0$ if $\delta_k < 0$.

B. Circular maneuvre C_k

Consider the case where step k is a turn C_k of radius R in the direction δ_k. Let $X_{k-1} = X_p(t_{k-1})$ denote the pursuer position at the end of the previous step and $X_k = X_p(t_k)$ at the end of the current one. By definition, one gets:

$$\alpha_k = \psi_k - \psi_{k-1} \tag{5}$$

Let us determine the final position X_k of the pursuer after the turn. According to triangular law for vector addition, the displacement can be decomposed as follows.

$$\overrightarrow{X_{k-1}X_k} = \overrightarrow{X_{k-1}O_k^{\delta_k}} + \overrightarrow{O_k^{\delta_k}X_k} \tag{6}$$

where $O_k^{\delta_k}$ is the center of 11111cs in the direction δ_k. As illustrated in Fig. 3, O_k^{δ} can be expressed as

$$O_k^{\delta_k} = X_{k-1} + R\begin{pmatrix}\cos\left(\psi_{k-1} + \delta_k\frac{\pi}{2}\right)\\ \sin\left(\psi_{k-1} + \delta_k\frac{\pi}{2}\right)\end{pmatrix}. \tag{7}$$

The position X_{k+1} can be expressed from $O_k^{\delta_k}$ as a point on a circle of radius R spanning the angle $\psi_k - \delta_k\frac{\pi}{2}$, as illustrated in Fig. 3. So:

$$X_{k+1} = O_k^{\delta_k} + R\begin{pmatrix}\cos\left(\psi_k - \delta_k\frac{\pi}{2}\right)\\ \sin\left(\psi_k - \delta_k\frac{\pi}{2}\right)\end{pmatrix}. \tag{8}$$

Using (6), (7) and (8), one gets

$$X_k = X_{k-1} + R\begin{pmatrix}\cos\left(\psi_{k-1} + \delta_k\frac{\pi}{2}\right) + \cos\left(\psi_k - \delta_k\frac{\pi}{2}\right)\\ \sin\left(\psi_{k-1} + \delta_k\frac{\pi}{2}\right) + \sin\left(\psi_k - \delta_k\frac{\pi}{2}\right)\end{pmatrix}. \tag{9}$$

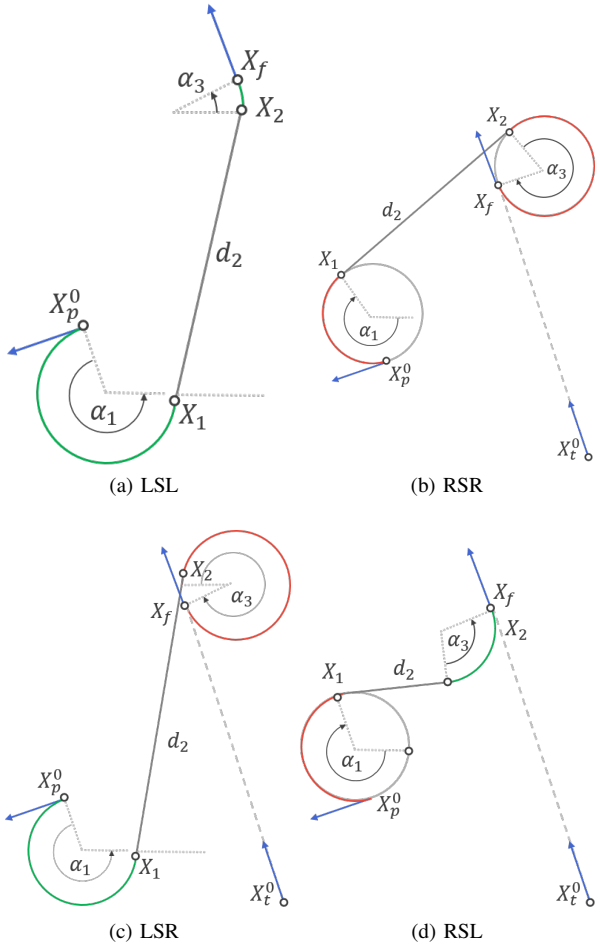

Fig. 2: The Four Dubins' Paths to intercept the target

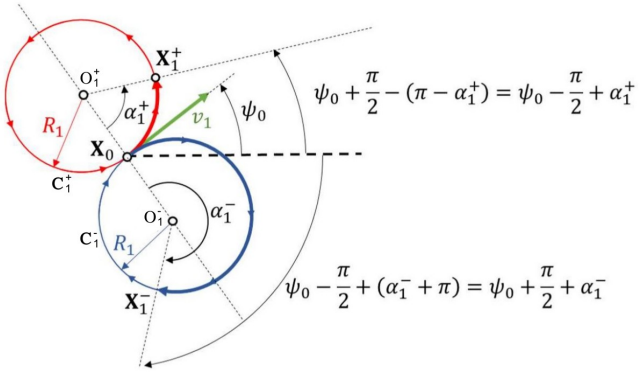

Fig. 3: First circular maneuvre

Finally, since the velocity v_p is constant, one gets the time t_k at the end of the rotation:

$$t_k = t_{k-1} + \frac{R}{v_p}\delta_k\alpha_k \tag{10}$$

The solution can be summarized with the following sys-

tem:

$$\begin{cases} \psi_k = \psi_{k-1} + \alpha_k \\ X_k = X_{k-1} + R\begin{pmatrix} \delta_k\left(-\sin\left(\psi_{k-1}\right) + \sin\left(\psi_k\right)\right) \\ \delta_k\left(\cos\left(\psi_{k-1}\right) - \cos\left(\psi_k\right)\right) \end{pmatrix} \\ t_k = t_{k-1} + \frac{R}{v_p}\alpha_k \end{cases} \tag{11}$$

C. Straight-line maneuvre S_k

Consider the case where step k corresponds to a straight line S_k. In this case, the heading is constant:

$$\psi_k = \psi_{k-1}. \tag{12}$$

Since the heading is constant, the vehicle moves from X_{k-1} following ψ_{k-1} for a distance d_k:

$$X_k = X_{k-1} + d_k \begin{pmatrix} \cos\left(\psi_{k-1}\right) \\ \sin\left(\psi_{k-1}\right) \end{pmatrix}. \tag{13}$$

Then, since the velocity is constant, one gets the arriving time t_k such that:

$$t_k = t_{k-1} + \frac{d_k}{v_p}. \tag{14}$$

The solution can be summarized with the following system:

$$\begin{cases} \psi_k = \psi_{k-1} \\ X_k = X_{k-1} + d_k \begin{pmatrix} \cos\left(\psi_{k-1}\right) \\ \sin\left(\psi_{k-1}\right) \end{pmatrix} \\ t_k = t_{k-1} + \frac{d_k}{v_p} \end{cases} \tag{15}$$

D. General solution

Based on the equations described in previous Sections III-B and III-C, the four CSC Dubins' Paths leading to the interception of the target by the pursuer can be expressed by the system exposed in Theorem 1.

Theorem 1: Consider a pursuer and its moving target whose dynamics are described respectively by (2) *and* (1)*. If the condition $v_p > v_t > 0$ is respected, for a fixed $\delta_1$and δ_3, the interception time t_f^δ induced by the four CSC Dubins' Paths leading to an interception is:*

$$t_f = t_0 + \frac{R}{v_p}(\delta_1\alpha_1 + \delta_3\alpha_3) + \frac{d_2}{v_p} \tag{16}$$

where the geometric parameters α_1, d_2 and α_3 are the solution of:

$$\begin{aligned} 0 = {} & (\delta_1 - \delta_3) \\ & \times R\left(\begin{bmatrix} \sin(\psi_0 + \alpha_1) \\ -\cos(\psi_0 + \alpha_1) \end{bmatrix} - \alpha_1 \frac{v_t}{v_p}\begin{bmatrix} \cos(\psi_t) \\ \sin(\psi_t) \end{bmatrix}\right) \\ & + d_2\left(\begin{bmatrix} \cos(\psi_0 + \alpha_1) \\ \sin(\psi_0 + \alpha_1) \end{bmatrix} - \frac{v_t}{v_p}\begin{bmatrix} \cos(\psi_t) \\ \sin(\psi_t) \end{bmatrix}\right) - A \end{aligned} \tag{17}$$

where A can be expressed as

$$\begin{aligned} A = {} & X_t^0 - X_p^0 - R\begin{bmatrix} -\delta_1\sin(\psi_0) + \delta_3\sin(\psi_t) \\ \delta_1\cos(\psi_0) - \delta_3\cos(\psi_t) \end{bmatrix} \\ & + v_t\begin{bmatrix} \cos\psi_t \\ \sin\psi_t \end{bmatrix}\left(\frac{\delta_3 R}{v_p}\left(\psi_3 - \psi_0\right)\right) \end{aligned} \tag{18}$$

$$\begin{aligned} \alpha_1 &= \psi_1 - \psi_0 \mod (2\pi) \\ \alpha_3 &= \psi_3 - \psi_1 \mod (2\pi) \end{aligned}$$

Proof of Theorem 1 can be found in [15][Appendix A.1].

Based on the paths defined in Theorem 1, the shortest path leading to the interception corresponds to the one with the smallest interception time t_f^δ, as exposed in Theorem 2.

Theorem 2: Consider the Dubins' Paths LSL, RSR, LSR and RSL exposed in Theorem1. Since the velocity of the vehicles is constant, the shortest path can be deduced by taking the minimal time between all four CSC paths interception time. The smallest interception t_f can so be expressed as

$$t_f = \min\left(t^{LSL}, t^{RSR}, t^{LSR}, t^{RSL}\right) \tag{19}$$

Note that one can deduce the corresponding interception position with $X_f = X_t^0 + v_t t_f \begin{bmatrix} \cos\left(\psi_t\right) \\ \sin\left(\psi_t\right) \end{bmatrix}$.

In practice, the analytical resolution of (17)-(18) is not always trivial. Yet, the explicit solutions in the *LSL* and *RSR* cases can be found and guarantees to find a path while, in the RSL and LSR cases, the use of an optimization tool might be necessary.

The explicit analytical resolution for case *RSR* and *LSL* will be provided in Section IV-A, while the implicit analytical resolution of LSR and RSL is exposed in Section IV-B

IV. Contribution: resolution of the system

A. Explicit analytical resolution of RSR and LSL

The *RSR* and *LSL* paths correspond to the specific case where $\delta_1 = \delta_3$, which allows strong simplification in the system 1. This leads to an explicit analytical solution of the problem described in the following theorem:

Theorem 3: Consider Theorem 1 with the specific case where $\delta_1 = \delta_3 = \delta$, i.e. the LSL and RSR paths. The interception time t_f^δ can be expressed as

$$t_f^\delta = t_0 + \frac{R}{v_p}\delta(\alpha_1 + \alpha_3) + \frac{d_2}{v_p} \tag{20}$$

with the geometric parameters α_1, d_2, α_3 as

$$\alpha_1 = \psi_1 - \psi_0 \mod (2\pi) \tag{21}$$

$$\alpha_3 = \psi_3 - \psi_1 \mod (2\pi) \tag{22}$$

$$d_2 = \frac{\|A\|^2}{\beta} \tag{23}$$

where β can be defined as

$$\begin{aligned} \beta = {} & -\frac{v_t}{v_p}\left\langle A, \begin{pmatrix} \cos\psi_t \\ \sin\psi_t \end{pmatrix}\right\rangle \\ & + \sqrt{\left(\frac{v_t}{v_p}\left\langle A, \begin{pmatrix} \cos\psi_t \\ \sin\psi_t \end{pmatrix}\right\rangle\right)^2 + \left(\frac{\|A\|}{v_p}\right)^2\left(v_p^2 - v_t^2\right)} \end{aligned} \tag{24}$$

with

$$\begin{aligned} A &= \left[A_x, A_y\right]^\top \\ &= X_t^0 - X_p^0 - R\delta\begin{bmatrix} -\sin\left(\psi_0\right) + \sin\left(\psi_t\right) \\ \cos\left(\psi_0\right) - \cos\left(\psi_t\right) \end{bmatrix} \\ &\quad - \frac{v_t}{v_p}R\delta\left(\psi_t - \psi_0\right)\begin{bmatrix} \cos\left(\psi_t\right) \\ \sin\left(\psi_t\right) \end{bmatrix}. \end{aligned} \tag{25}$$

Details of the proof are exposed in [15][Appendix A.2]. In particular, it is proved that d_2 exists as $v_p > v_t$.

B. Implicit analytical resolution of LSR and RSL

Consider now the case where $\delta_1 = -\delta_3$. The system 1 can be simplified as described in Theorem 4.

Theorem 4: Consider the Theorem 1 with the specific case where $\delta_1 = \delta_3 = \delta$, i.e. the path LSL and RSR. The interception time t_f^δ can be expressed as

$$t_f = t_0 + \frac{R}{v_p}\delta(\alpha_1 - \alpha_3) + \frac{d_2}{v_p} \tag{26}$$

with the geometric parameters α_1, d_2, α_3 linked by the relations:

$$\begin{aligned} 0 = 2R\delta &\left(\begin{bmatrix} \sin(\psi_0 + \alpha_1) \\ -\cos(\psi_0 + \alpha_1) \end{bmatrix} - \alpha_1 \frac{v_t}{v_p} \begin{bmatrix} \sin\psi_t \\ \cos\psi_t \end{bmatrix} \right) \\ + d_2 &\left(\begin{bmatrix} \cos(\psi_0 + \alpha_1) \\ \sin(\psi_0 + \alpha_1) \end{bmatrix} - \frac{v_t}{v_p} \begin{bmatrix} \cos\psi_t \\ \sin\psi_t \end{bmatrix} \right) - A \end{aligned} \tag{27}$$

where A can be expressed as

$$\begin{aligned} A = X_t^0 - X_p^0 - R\delta &\begin{bmatrix} -\sin\psi_0 - \sin\psi_t \\ \cos\psi_0 + \cos\psi_t \end{bmatrix} \\ - R\delta \frac{v_t}{v_p}(\psi_3 - \psi_0) &\begin{bmatrix} \cos\psi_t \\ \sin\psi_t \end{bmatrix}) \end{aligned} \tag{28}$$

$$\begin{aligned} \alpha_1 &= \psi_1 - \psi_0 \mod (2\pi) \\ \alpha_3 &= \psi_3 - \psi_1 \mod (2\pi) \end{aligned}$$

Detail of the proof in [15][Appendix A.3].

Note that (27) is implicit and requires a numerical resolution to compute ψ_1 and d_2 independently.

C. Discussion

We can observe that the RSR and LRL paths have an analytical solution, whereas the RSL and LSR paths require numerical resolution. Since analytical resolution provides a solution with much lower computational time and resource requirements, it may be advantageous to restrict the choice of paths to RSR and LRL for real-time implementations on low-power or highly reactive computing platforms. Similarly, this choice becomes even more relevant when integrating the method into larger computational architectures, such as path planning, probabilistic methods, or more generally in iterative, exhaustive, or brute-force algorithms. The explicit analytical expression can also be used for the computation of the state Jacobian, thereby opening up additional possibilities for control. Once the path and the position and time of the interception (X_f, t_f) have been determined using the method, the vehicle's velocity can be adjusted to avoid moving obstacles that may cross its path. A combination of acceleration and deceleration can thus be applied, as long as the vehicle reaches the intersection point X_f at the specified time t_f.

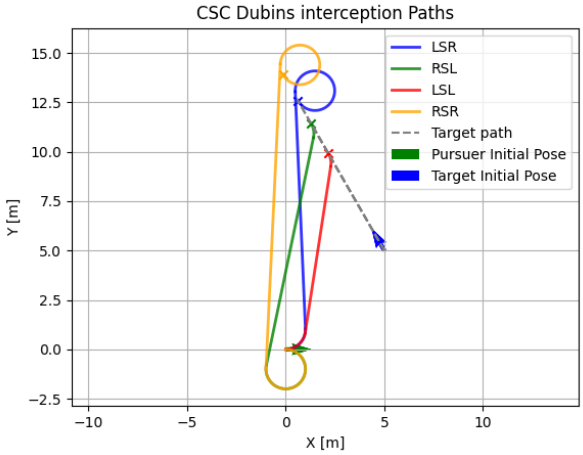

Fig. 4: CSC Dubins Interception paths

path type	mean	std	median 50%
LSL	0.001	0.002	0.011
RSR	0.010	0.002	0.010
LSR	0.183	0.09	0.159
RSL	0.172	0.274	0.161

TABLE I: Comparison of 10.000 execution time in ms per path type

V. Results

A. Simulations

To test the results, simulations have been conducted. Fig. 4 illustrates the four Dubins' Paths to intercept the target in different colors computed according to previous expressions.

Fig. 5 and Table I display a comparison of computation times in ms between explicit expressions LSL and RSR and implicit LSR and RSL ones. The test was conducted in Python on 10,000 target positions regularly distributed on a 100×100 grid, using a 2.4 GHz Intel Core i7 13th Gen CPU running Ubuntu 22.04 in idle mode (no background applications). The difference in computing time is due to the use of solver for the implicit paths.

While in the present context this difference can be considered negligible — since the calculation is performed only once and the boat's dynamics are much slower than the computation time — this is not the case when using Dubins paths in an iterative, exhaustive, or brute-force algorithm, where the user needs to compute paths a very large number of times. In such cases, the explicit expressions of the RSR and LSL paths allow for an implementation that is up to a hundred times faster, making them significantly more efficient and attractive.

B. Experiment

1) Experiment description: The experiment took place at Lake Guerledan, Brittany, France. It was conducted with two BlueBoats[1], both equipped with a GNSS. Both BlueBoats

[1]https://bluerobotics.com/store/boat/blueboat/blueboat/

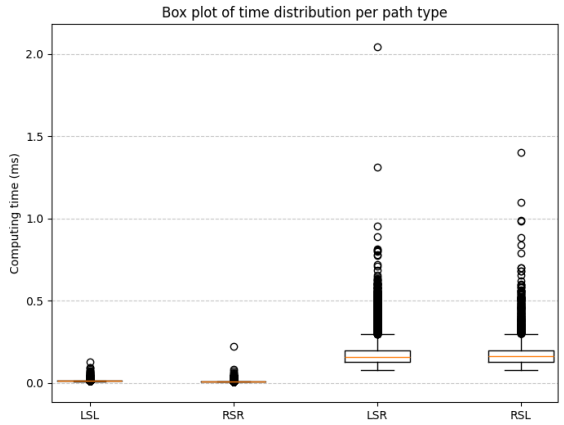

Fig. 5: Boxplot of execution time per path type

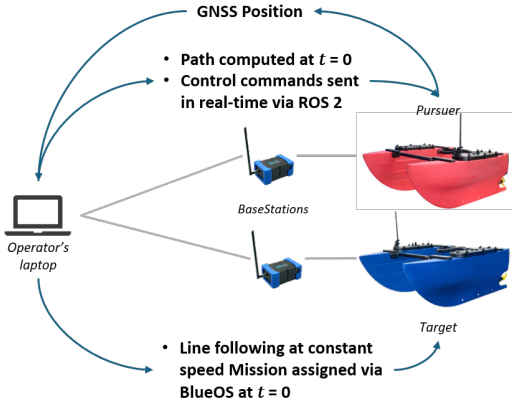

Fig. 6: Experiment scheme

were connected to their own wireless base station. The target had a simple straight line to follow at a speed $v_t = 1m.s^{-1}$. Its mission is planned using QGroundControl software. Fig. 6 illustrates the experiment setup.

We suppose here that the pursuer knows the initial position of the target and its orientation.

2) Experimental results: Since the explicit formulation of the *LSL* and *RSR* paths constitutes the core of this work, we apply an *LSL* path in our experiment to validate the interception in practice without focusing on optimizing the interception time. The evaluation of the other paths is presented in Section V-A. A video is available here[2]. Fig. 7 shows the pursuer intercepting the target in real conditions. Fig. 8 represents the paths followed by the vehicles during the interception mission.

The pursuer intercepts the moving target by following the Dubins path computed with our formulation, while path tracking is ensured by the controller proposed in [16]. No replanning is performed during the mission. Advanced positioning accuracy relying on RTK GNSS would further improve the results. The u-blox M9 standard precision GNSS

[2]https://youtu.be/pAslI3rbxes

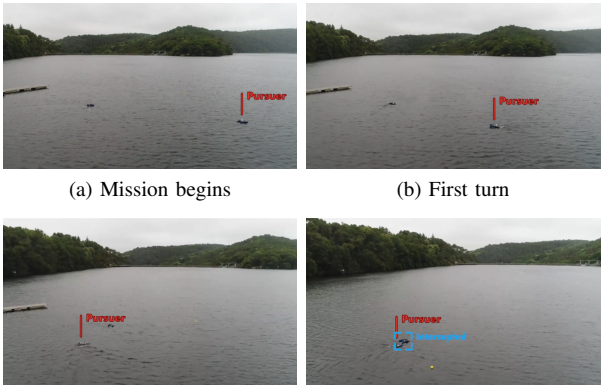

(a) Mission begins (b) First turn

(c) Straight line into second turn (d) Target Intercepted

Fig. 7: Experiment performed with two Blueboats.

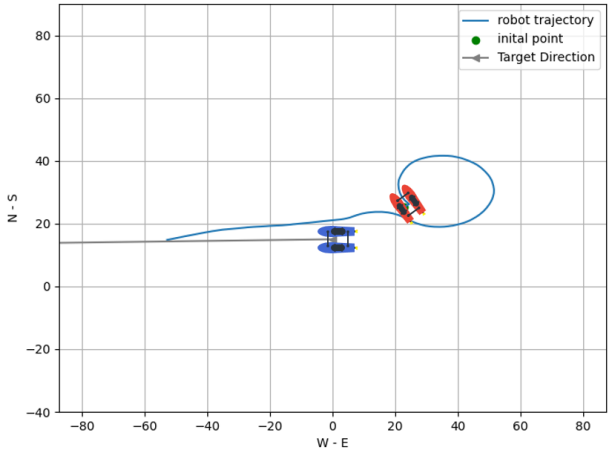

Fig. 8: Position of the target and pursuer during the interception experiment. Gray line is the path followed by the target at a constant speed, Blue line is the path of the pursuer.

platform, can deliver meter-level accuracy as claimed in [17].

VI. Conclusion

This work presents an explicit analytical solution for a rendezvous problem using the CSC Dubins' Paths, enabling real-time determination of the fastest path to reach the target with the same final heading. Additionally, this work is validated experimentally through tests conducted on USVs.

Future work will focus on extending the results to CCC paths and deriving explicit formulas for the LSR and RSL cases. The generalization to 3D vehicle dynamics is also a promising direction for further investigation. Ultimately, this work is intended for application in underwater docking scenarios where two AUVs maintain a constant depth during convergence, before executing the final docking maneuver.

References

[1] P. Gong, H. Zhang, F. Xu, G. Pan, Z. Yan, and D. Zhang, "Mpc-based docking control between uuv and mobile mothership," in *2023 7th CAA Int. Conf. on Vehicular Control and Intelligence (CVCI)*, 2023, pp. 1–5.

[2] N. Dahn *et al.*, "Autonomous docking between a mobile subsea docking station and an auv while in motion," in *OCEANS 2024 - Halifax*, 2024, pp. 1–9.
[3] S. M. LaValle, "Motion planning," *IEEE Robotics & Automation Magazine*, vol. 18, no. 2, pp. 108–118, 2011.
[4] L. E. Dubins, "On curves of minimal length with a constraint on average curvature, and with prescribed initial and terminal positions and tangents," *American Journal of Mathematics*, vol. 79, no. 3, pp. 497–516, 1957.
[5] J. A. Reeds and L. A. Shepp, "Optimal paths for a car that goes both forwards and backwards," *Pacific Journal of Mathematics*, vol. 145, no. 2, pp. 367–393, 1990.
[6] L. S. Pontryagin, V. G. Boltyanskii, R. V. Gamkrelidze, and E. F. Mishchenko, *L. S. Pontryagin Selected Works, Volume 4: The Mathematical Theory of Optimal Processes*. Montreux, Switzerland: Gordon and Breach, 1986.
[7] J.-D. Boissonnat, A. Cerezo, and J. Leblond, "Shortest paths of bounded curvature in the plane," in *Proc. IEEE Int. Conf. on Robotics and Automation (ICRA)*, vol. 3, Nice, France, 1992, pp. 2315–2320.
[8] M. Owen, R. W. Beard, and T. W. McLain, "Implementing dubins airplane paths on fixed-wing uavs," in *Handbook of Unmanned Aerial Vehicles*. Springer, 2014, pp. 1677–1701.
[9] P. Váña, A. A. Neto, J. Faigl, and D. G. Macharet, "Minimal 3d dubins' path with bounded curvature and pitch angle," in *2020 IEEE Int. Conf. on Robotics and Automation (ICRA)*, 2020, pp. 8497–8503.
[10] M. Moll, "3d dubins' paths for underwater vehicles," in *Proc. IEEE/MTS Oceans Conf.*, Halifax, Canada, 2024.
[11] Y. Meyer, P. Isaiah, and T. Shima, "On dubins' paths to intercept a moving target," *Automatica*, vol. 53, pp. 256–263, Mar. 2015.
[12] S. Manyam, D. W. Casbeer, A. von Moll, and Z. Fuchs, "Shortest dubins' paths to intercept a target moving on a circle," *J. Guid., Control, Dyn.*, vol. 45, no. 7, pp. 1–14, Jul. 2022.
[13] J. A. Morgan, "Interception in differential pursuit/evasion games," arXiv preprint arXiv:1103.2063, 2011.
[14] U. Vautier, C. Viel, J. Wan, L. Jaulin, R. Hone, and M. Dai, "Restricted orientation dubins' path with application to sailboats," *IEEE Robot. Autom. Lett.*, vol. 4, no. 4, pp. 4515–4522, 2019.
[15] [Online]. Available: https://tbelier.github.io/assets/publications/ICRA2026Appendix.pdf
[16] L. Lapierre and D. Soetanto, "Nonlinear path-following control of an auv," *Ocean Engineering*, vol. 34, no. 11, pp. 1734–1744, 2007. [Online]. Available: https://www.sciencedirect.com/science/article/pii/S0029801807000406
[17] [Online]. Available: https://www.tinytronics.nl/product_files/004333_NEO-M9N00B_DataSheet_UBX19014285.pdf